THE ASTRONOMICAL JOURNAL VOLUME 111, NUMBER 4 APRIL 1996

RADII AND EFFECTIVE TEMPERATURES FOR K AND M GIANTS AND SUPERGIANTS

H. M. DYCK[1]
Department of Physics and Astronomy, University of Wyoming, Laramie, Wyoming 82071
Electronic mail: meldyck@uwyo.edu

J. A. BENSON[1]
NPOI, U.S. Naval Observatory, 1400 W. Mars Hill Road, Flagstaff, Arizona 86001
Electronic mail: benson@lowell.edu

G. T. VAN BELLE
Department of Physics and Astronomy, University of Wyoming, Laramie, Wyoming 82071
Electronic mail: vanbelle@uwyo.edu

S. T. RIDGWAY
National Optical Astronomy Observatories, P.O. Box 26732, Tucson, Arizona 85726
Electronic mail: ridgway@noao.edu

Received 1995 September 12; revised 1995 November 13

ABSTRACT

Interferometrically determined angular diameters for 37 K0−M8 giant and supergiant stars are presented in this paper. It is shown that the effective temperatures determined for this sample agree with previous determinations made at CERGA and by occultations and that there is no significant difference among the effective temperature scales set by the three investigations. The effective temperature data from the three sources are combined to give a new mean relationship between effective temperature and spectral type extending to spectral types as late as M7, where the precision is approximately ±95 K at each spectral type. The question of the natural dispersion in the effective temperature scale is discussed and found to lie between ±40 and ±80 K. Several new supergiants have been observed and a previous suggestion is confirmed that the supergiant temperature scale is cooler than the corresponding scale for giants. The difference in temperature between the two luminosity classes decreases with decreasing temperature. Linear radii for 22 stars have been computed by combining the angular diameter data with the best available parallax data. The middle M giants have radii approximately 80 times the Solar radius.

1. INTRODUCTION

One of the last observational problems in stellar atmospheres is the detailed study of the surface structure of a star. The lowest-order measurable parameter of surface structure, the overall size, is necessary for the determination of the stellar effective temperature. In the H–R diagram, the coolest region is the least well constrained by observation. K–M luminosity class I–III stars are common and potentially useful in galactic structure studies, as distance indicators, so that their properties ought to be well understood. Two decades ago began a renaissance in the study of stellar angular diameters, with the development of speckle interferometry, lunar occultation studies, and Michelson interferometers. Significant steps were made to delineate the effective temperature scale for cool stars by Ridgway *et al.* (1980), DiBenedetto & Rabbia (1987), DiBenedetto & Ferluga (1990), and DiBenedetto (1993), using observations made primarily at near-infrared wavelengths. Forty-four stars were used in these analyses.

In 1990 we began a program to measure angular diameters for a large sample of cool stars. To date, the only results which have been published are for α^1 Her (Benson *et al.* 1991), for α Ori (Dyck *et al.* 1992) and for RX Boo and RS Cnc (Dyck *et al.* 1995). Owing to the completion of the first phase of construction of IOTA (the Infrared Optical Telescope Array) and to improvements in the operating efficiency, we are now in a position to increase this sample manyfold. Here, we report new observations of 34 K0−M8 stars of luminosity class I, II, and III and we rediscuss data for an additional three stars already published. We are concentrating our observations at near-infrared wavelengths for several reasons. First, these stars radiate most of their energy at the longer wavelengths. Second, it allows us to compare our results more directly to the previous determinations of effective temperature, referenced above, and thus provide a more homogeneous set for understanding the astrophysical parameters for these stars. Third, and most important, it is well known that many stars of this late type show the obser-

[1]Visiting scientist at the National Optical Astronomy Observatories.

 0004-6256/96/111(4)/1705/8/$6.00

TABLE 1. The program stars.

BS	Name	Spectral Type	Ref	A_V	F_{TOT} (W cm^{-2})
2061	α Ori	M1-2Ia-Ib	1	0.46	1.15×10^{-11}
3639	RS Cnc	M6III(S)	2	0.46	8.47×10^{-13}
4909	TU Cvn	M5-III	1	0.0	2.21×10^{-13}
5299	BY Boo	M4.5III	1	0.0	2.55×10^{-13}
5340	α Boo	K1.5III	1	0.34	5.83×10^{-12}
....	RX Boo	M7.5-8	1	0.0	8.85×10^{-13}
5512	HD130144	M5IIIab	2	...	3.82×10^{-13}
....	τ^4 Ser	M5IIIa	1	0.0	4.20×10^{-13}
....	ST Her	M6-7III(S)	1	...	3.72×10^{-13}
....	X Her	M7	3	0.0	6.05×10^{-13}
6056	δ Oph	M0.5III	1	0.0	7.58×10^{-13}
6146	g Her	M6-III	1	0.0	1.08×10^{-12}
6406	α^1 Her	M5Ib-II	1	0.0	4.34×10^{-12}
6702	OP Her	M5IIb-IIIa	4	0.0	1.64×10^{-13}
6705	γ Dra	K5III	1	0.0	9.06×10^{-13}
7009	XY Lyr	M4.5-5+II	1	0.0	2.26×10^{-13}
7139	δ^2 Lyr	M4II	1	0.0	5.79×10^{-13}
7157	R Lyr	M5III	2	0.0	1.23×10^{-12}
7525	γ Aql	K3II	1	0.37	5.53×10^{-13}
7536	δ Sge	M2II	2	0.0	4.32×10^{-13}
7635	γ Sge	M0-III	1	0.0	3.24×10^{-13}
7645	VZ Sge	M4IIIa	2	...	2.30×10^{-13}
7735	31 Cyg	K4Ib	5	0.0	1.75×10^{-13}
7751	32 Cyg	K5Iab	5	0.0	2.11×10^{-13}
7886	EU Del	M6III	1	0.0	5.03×10^{-13}
7941	U Del	M5II-III	6	0.0	2.83×10^{-13}
7951	EN Aqr	M3III	1	0.0	2.52×10^{-13}
8062	HD200527	M4.5III(S)	1	0.0	8.42×10^{-14}
8079	ξ Cyg	K4.5Ib-II	1	0.34	2.91×10^{-13}
....	V1070 Cyg	M7III	7	...	3.07×10^{-13}
8262	W Cyg	M5IIIa	2	0.0	5.88×10^{-13}
8308	ε Peg	K2Ib-II	1	0.58	7.83×10^{-13}
....	TW Peg	M6-7	8	...	3.18×10^{-13}
....	SV Peg	M7	8	...	2.78×10^{-13}
....	RX Lac	M6	8	...	2.27×10^{-13}
8698	λ Aqr	M2.5III	1	0.0	4.03×10^{-13}
8775	β Peg	M2.5II-III	1	0.0	1.63×10^{-12}

References for spectral types used in Table 1: (1) Keenan & McNeil (1989), (2) Hoffleit (1982), (3) Lockwood (1972), (4) Keenan (1963), (5) Wright (1970), (6) Keenan (1942), (7) Moore & Paddock (1950), (8) Kukarkin et al. (1969).

vational effects of circumstellar dust shells. Tsuji (1978) pointed out that the dust is often hard to separate from the photosphere, making a determination of the photospheric diameter problematic. At optical wavelengths, the dust particles can scatter the stellar radiation while in the thermal infrared the dust reradiates absorbed stellar energy. Light at near-infrared wavelengths, on the other hand, will penetrate to the stellar photosphere.

The selection of sources was governed by expected angular size, based upon blackbody calculations, and availability. The stars observed here are mostly in the spring and summer parts of the sky. We did not include in the sample any known Mira variables or stars with optically thick circumstellar shells. The sources are listed in Table 1, where we give the *Bright Star Catalog* number (Hoffleit 1982), an alternate designation, the adopted spectral type, the source for that spectral type, the assumed interstellar reddening, and the bolometric flux.

Using the data reported in this paper, along with the published occultation and Michelson interferometry data, we assemble a sample of 80 independent observations of K and M giant and supergiant stars, with spectral classes extending to M8. We show that the effective temperature scales previously established are correct and extend them to later spectral types. For the first time, we have enough stars to assess the spread in effective temperatures within a spectral subtype and evaluate the natural width of the effective temperature scale for a given spectral type. The comparison of effective temperature scales for giants and supergiants is readdressed (Dyck *et al.* 1992), with the conclusion that supergiants are indeed systematically cooler at a given spectral type. Finally, we look at the linear radii for the few stars which have accurate parallax data.

2. OBSERVATIONS

The new data reported in this paper were obtained in the K (λ=2.2 μm, $\Delta\lambda$=0.4 μm) filter with IOTA. The interferometer, detectors, and data reduction procedures have been described more fully by Carleton *et al.* (1994) and Dyck *et al.* (1995). IOTA is presently operated in a two-telescope configuration and infrared observations were made on 31 nights during 1993, 1994, and 1995. Completion of the vacuum delay system during the summer and fall of 1994 has made possible the use of all available baselines, although only two, 21 and 38 m, were used for the observations reported herein. We sweep the optical delay line past the white light fringe position at a rate which produces an interferogram with a fringe frequency of 100 Hz. The data-collection window is sufficiently long that all of the interference pattern from a source (the interferogram) is recorded as the optical delay line sweeps past the white light position. The beams from the two telescopes are combined onto a beamsplitter, producing a reflected and transmitted component for each telescope. Thus, two independent interference signals may be recorded simultaneously for each object observed. Improvements made to the data-taking computers and software during 1994–1995 routinely allow us to obtain 1500–2000 interferograms in each data channel in an 8 hr night.

The interferograms are digitally filtered with a 100 Hz square bandpass filter and normalized by the total flux from the source. For a perfect optical system, the amplitude of this normalized interferogram (called the visibility amplitude or simply the visibility) is directly related to the angular diameter of a partially resolved stellar disk, in the sense that smaller visibility amplitudes correspond to larger angular sizes. An unresolved source will have unit visibility. However, alignment errors and other system aberrations will reduce this point source response below unity. Therefore, observations of program stars are interleaved with observations of unresolved calibration stars in order to determine the interferometer point-source response and to minimize the effects of its variations. Stellar calibration sources were chosen on the basis of blackbody calculations from the star's known spectral type and observed flux. We tried to restrict our se-

TABLE 2. Calibrated visibilities in the two channel data.

Star	UT Date	B(m)	V_0	ε_0	V_1	ε_1	Star	UT Date	B(m)	V_0	ε_0	V_1	ε_1
γ Aql	95Jun09	35.74	0.508	0.001	0.454	0.004	g Her	95Apr30	20.67	0.644	0.039	0.573	0.030
γ Aql	95Jun10	35.80	0.616	0.028	0.600	0.023	g Her	95May01	20.82	0.535	0.018	0.462	0.016
γ Aql	95Jun11	36.07	0.710	0.067	.....	.....	OP Her	95Jun04	37.44	0.775	0.003	0.797	0.019
γ Aql	95Jun12	36.14	0.782	0.033	0.612	0.021	OP Her	95Jun05	37.50	0.753	0.007	0.779	0.005
λ Aqr	95Jul11	31.12	0.604	0.076	.....	.....	ST Her	95Jun03	36.90	0.481	0.005	0.462	0.013
EN Aqr	95Jul08	36.32	0.777	0.025	0.781	0.062	ST Her	95Jun04	36.92	0.431	0.011	0.387	0.011
α Boo	94May19	21.14	.....	.....	0.329	0.035	ST Her	95Jun05	36.89	0.435	0.016	0.436	0.011
α Boo	94May20	21.14	.....	.....	0.259	0.005	X Her	95Apr29	20.44	0.687	0.018	0.671	0.002
3Y Boo	95Jun03	37.36	0.713	0.001	0.700	0.010	X Her	95May01	20.25	0.687	0.004	0.594	0.003
3Y Boo	95Jun04	37.23	0.641	0.009	0.593	0.013	X Her	95Jun03	37.50	0.193	0.002	0.180	0.003
3Y Boo	95Jun05	37.29	0.692	0.001	0.616	0.016	X Her	95Jun04	37.18	0.220	0.001	0.220	0.008
RX Boo	94Jan21	21.13	0.239	0.019	0.238	0.013	RX Lac	95Jul10	37.40	0.622	0.038	0.821	0.046
RX Boo	94Apr19	21.21	0.443	0.018	0.381	0.018	δ^2 Lyr	94Apr19	21.12	0.895	0.039	0.772	0.044
RX Boo	94May05	21.15	0.509	0.026	0.472	0.038	δ^2 Lyr	94May05	21.23	0.862	0.039	0.997	0.048
RX Boo	94May19	21.21	.....	.....	0.253	0.029	δ^2 Lyr	95Jun05	37.63	0.370	0.006	0.356	0.008
RX Boo	94May20	21.12	.....	.....	0.165	0.002	δ^2 Lyr	95Jul09	37.26	0.372	0.011	0.373	0.001
RX Boo	94Jun02	21.19	.....	.....	0.259	0.017	R Lyr	95Apr29	20.70	0.572	0.012	0.482	0.015
RX Boo	94Jun03	21.12	.....	.....	0.316	0.005	R Lyr	95Apr30	20.71	0.689	0.006	0.610	0.001
RS Cnc	93Dec10	21.21	0.713	0.032	0.701	0.024	R Lyr	95May01	20.53	0.704	0.031	0.618	0.026
RS Cnc	94Jan14	21.21	0.436	0.029	0.512	0.027	XY Lyr	95Jun02	37.59	0.590	0.007	0.647	0.015
RS Cnc	94Jan20	21.21	0.528	0.057	0.402	0.053	XY Lyr	95Jun03	37.00	0.663	0.010	0.660	0.011
RS Cnc	94Jan21	21.21	0.417	0.041	0.422	0.016	XY Lyr	95Jun04	37.10	0.676	0.003	0.712	0.016
RU CVn	95Jul10	37.40	0.564	0.041	0.642	0.049	δ Oph	95Jun13	35.82	0.477	0.028	0.488	0.028
W Cyg	95Jun02	36.84	0.270	0.028	0.369	0.050	δ Oph	95Jul12	29.97	0.598	0.027	0.575	0.039
W Cyg	95Jun05	36.75	0.179	0.003	0.171	0.002	β Peg	93Dec10	21.18	0.485	0.033	0.489	0.036
ξ Cyg	95Jul10	37.82	0.499	0.033	0.680	0.019	β Peg	94Jun09	21.21	0.689	0.038	0.510	0.032
1070 Cyg	95Jun04	37.21	0.584	0.003	0.655	0.009	ε Peg	95Jun12	36.70	0.622	0.022	0.559	0.042
1070 Cyg	95Jun05	36.76	0.573	0.001	0.584	0.001	ε Peg	95Jul06	36.64	0.618	0.015	.....	.....
31 Cyg	95Jul10	37.42	0.671	0.0601	0.7943	0.066	ε Peg	95Jul07	36.52	0.664	0.021	0.696	0.005
32 Cyg	95Jul10	37.29	0.647	0.057	0.776	0.069	SV Peg	95Jul10	37.13	0.460	0.030	0.603	0.048
EU Del	95Jun10	36.90	0.372	0.018	0.437	0.010	TW Peg	95Jul09	37.38	0.447	0.008	0.491	0.012
EU Del	95Jun11	36.99	0.346	0.069	.....	.....	δ Sge	95Jun07	36.86	0.653	0.016	0.650	0.011
EU Del	95Jun12	36.93	0.394	0.004	0.483	0.014	δ Sge	95Jun09	36.79	0.560	0.015	0.531	0.016
U Del	95Jul06	36.84	0.570	0.009	.....	.....	δ Sge	95Jun10	36.86	0.514	0.013	0.578	0.013
U Del	95Jul07	36.60	0.562	0.001	0.604	0.009	γ Sge	95Jun11	36.99	0.835	0.042	.....	.....
γ Dra	95Jun02	36.73	0.596	0.011	0.533	0.008	VZ Sge	95Jun12	36.81	0.856	0.025	0.985	0.061
γ Dra	95Jun03	36.68	0.409	0.001	0.371	0.008	τ^4 Ser	95Jun07	35.75	0.437	0.001	0.480	0.006
γ Dra	95Jun04	36.76	0.407	0.018	0.465	0.022	τ^4 Ser	95Jun09	35.78	0.410	0.004	0.401	0.002
γ Dra	95Jun05	36.66	0.325	0.0122	0.252	0.015	τ^4 Ser	95Jun10	35.91	0.389	0.010	0.430	0.007
g Her	95Apr28	20.84	0.493	0.025	0.414	0.024	BS5512	95Jun10	36.62	0.587	0.006	0.600	0.021
g Her	95Apr29	20.68	0.584	0.011	0.532	0.024	BS5512	95Jun13	36.52	0.589	0.004	0.542	0.004
							BS8062	95Jul10	37.62	0.925	0.052	0.987	0.080

lection to sources with visibilities greater than 90%, so that errors in these estimates, that propagate to the program star visibilities, would be minimized. The amplitude of a filtered source interferogram is determined and divided by the corresponding amplitude for a calibrator interferogram, to remove the point source response of the instrument. The resulting ratio is the properly calibrated visibility amplitude for the source. In Table 2 we list the observed data, where we give the date of the observation, the interferometer projected baseline, the mean visibility amplitude in each of the two detector channels, obtained from multiple interferograms, and the standard deviation of the mean for each channel.

We noted earlier (Dyck *et al.* 1995) that the interferometer internal consistency on a given night was better than that for repeated observations over more than one night. We now have a sufficient body of repeated nightly observations to quantify that difference: For a source which is about 50% resolved, the standard deviation for a single night's observation in one data channel is ±0.072. Although we do not yet fully understand the reasons for the differences, they apparently arise from small changes in the instrument response which are incompletely calibrated out by the observation of unresolved sources. Because these night-to-night, external, errors are larger than the errors listed in Table 2, we adopt them as a better estimate of the true precision of the visibility observations. For the purpose of computing the angular diameters and effective temperatures, we have averaged the visibility data in Table 2 and assigned an error based upon

TABLE 3. The derived data.

Star	θ_{UD} (mas)	ε_θ (mas)	θ_R (mas)	T_{EFF} (K)	ε_T (K)
α Ori	44.2	0.2	45.2	3605	43
RS Cnc	14.8	0.5	15.1	3246	67
TU CVn	7.4	0.6	7.6	3281	139
BY Boo	6.8	0.3	6.9	3547	89
α Boo	19.1	1.0	19.5	4628	133
RX Boo	18.4	0.5	18.8	2943	53
BS5512	7.9	0.4	8.1	3641	102
τ^4 Ser	9.8	0.3	10.0	3348	65
ST Her	9.3	0.3	9.5	3334	67
X Her	12.1	0.4	12.4	3300	67
δ Oph	9.3	0.5	9.5	3983	117
g Her	14.9	0.5	15.2	3438	71
α^1 Her	33	0.5	33.7	3271	46
OP Her	5.4	0.5	5.5	3565	170
γ Dra	9.6	0.3	9.8	4099	80
XY Lyr	6.8	0.3	6.9	3442	86
δ^2 Lyr	9.6	0.4	9.8	3665	88
R Lyr	13.3	0.6	13.6	3759	96
γ Aql	7.6	0.3	7.8	4072	94
δ Sge	7.8	0.3	8.0	3779	85
γ Sge	4.6	1.1	4.7	4579	550
VZ Sge	3.2	1.1	3.3	5039	868
31 Cyg	5.9	0.6	6.0	3466	181
32 Cyg	6.2	0.6	6.3	3543	176
EU Del	9.7	0.4	9.9	3520	84
U Del	7.9	0.5	8.1	3378	114
EN Aqr	5.5	0.7	5.6	3933	255
BS8062	2.3	1.1	2.4	4624	1107
ξ Cyg	7.5	0.6	7.7	3491	146
V1070 Cyg	7.6	0.4	7.8	3515	101
W Cyg	11.5	0.4	11.8	3361	71
ε Peg	7.3	0.4	7.5	4532	135
TW Peg	8.9	0.6	9.1	3277	117
SV Peg	8.3	0.6	8.5	3281	125
RX Lac	6.1	0.6	6.2	3638	184
λ Aqr	8.9	1.0	9.1	3477	200
β Peg	14.3	0.7	14.6	3890	106

the formula

$$\epsilon_V = \pm \frac{0.072}{\sqrt{(\text{Number of Nights}) \times (\text{Number of Data Channels})}}. \quad (1)$$

We computed average baselines and unweighted mean visibilities and assigned the standard errors based upon this formula. In Table 3, we list the uniform disk angular diameter, θ_{UD}, in milliarcseconds (mas), computed by fitting the Bessel function J_1 to the mean visibility at the baseline. When stars were observed on more than one baseline (i.e., when there was more than about 5% difference in the baseline), angular diameters and errors were computed for each baseline and only the weighted mean angular diameter and its weighted error are given in Table 3. We have also included previously published data for α^1 Her (Benson *et al.* 1991), α Ori (Dyck *et al.* 1992), and RS Cnc (Dyck *et al.* 1995). RX Boo is also repeated because new observations were obtained in 1994.

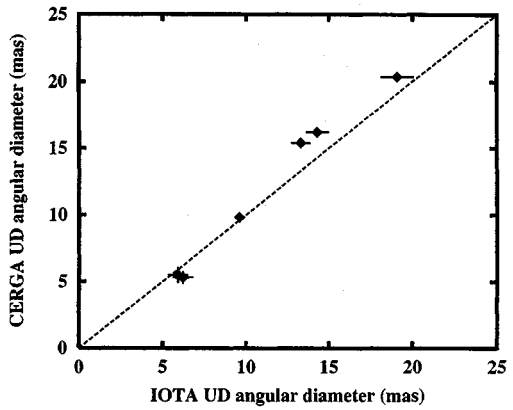

FIG. 1. A comparison of the uniform disk angular diameters determined with IOTA and CERGA, for six stars measured in common. The dashed line delineates the equal-diameter locus.

There are six stars—α Boo, γ Dra, R Lyr, β Peg, 31 Cyg, and 32 Cyg—which have been measured both at IOTA and at CERGA, but with different approaches to the fringe visibility detection. A comparison of the uniform-disk angular diameters is shown plotted in Fig. 1. From the plot, one can see that the measurements of the three stars with $\theta_{UD} \leq 10$ mas agree well. However, the measurements of the three larger stars differ, in the sense that the IOTA diameters are, on average, 90% of the CERGA diameters. For these larger stars, we have also compared the visibility measurements directly, in addition to the uniform-disk diameters and there clearly is a systematic difference between the data sets. Six stars measured in common are too few to allow us to decide whether there is a general systematic difference or simply the statistics of small numbers at work. We note that a 10% error in the angular size results in a 5% error in the effective temperature scale.

3. EFFECTIVE TEMPERATURES

We have been careful to choose, where possible, stars that are classified on the MK system, preferring spectral types estimated by Keenan and his co-workers. Second choices have been spectral types from Hoffleit (1982) and Lockwood (1972), both of which correlate very well with the Keenan types. In a few cases, other alternative sources were necessary. Total flux densities were obtained from magnitudes published in references in the SIMBAD database and in Gezari *et al.* (1993). We have estimated the effects of interstellar reddening by using the observed and intrinsic colors for the

spectral type (Johnson 1966; Schmidt-Kaler 1982). Reddening corrections for each wavelength were obtained from van de Hulst's theoretical reddening curve number 15 (see Johnson 1968). There is very little difference between this theoretical curve and the empirical reddening determination made by Mathis (1980). Monochromatic flux densities at each wavelength were obtained from the magnitudes using absolute calibrations by Hayes & Latham (1975), Hayes (1984), and Blackwell *et al.* (1983). Bolometric flux densities were generally computed from a simple numerical integration of the observed monochromatic flux densities from 0.45 to 5 μm. Flux contributions beyond 5 μm were estimated by integrating a Rayleigh–Jeans distribution, normalized to the 5 μm flux density. For eight stars, not enough data were found to carry out a complete bolometric flux density integration. In this case the mean relationship between flux density at K (2.2 μm) and total flux as a function of spectral type (Dyck *et al.* 1974) was used to estimate the bolometric flux density.

In order to compute the effective temperature, it is necessary to convert the uniform-disk angular diameters to limb-darkened diameters through the use of model atmospheres. It has been noted that these corrections are generally small in the infrared, so that errors will not greatly affect the results (see, for example, DiBenedetto 1993). As we have done in the past (Dyck *et al.* 1995), we used the models of Scholz & Takeda (1987) to compute these numerical correction factors. Following the suggestion of Scholz (1985) we compute a fictitious angular diameter θ_R, corresponding to the level in the atmosphere where the Rosseland mean opacity is unity. These corrections are nearly independent of spectral type over the range of temperatures and luminosity classes considered here and have a mean value $\theta_R \approx 1.022\ \theta_{\rm UD}$. We have adopted this conversion for all stars observed in this study. This correction factor is approximately the same as those used for the CERGA and occultation results, so that our results and theirs may be directly compared.

The effective temperatures $T_{\rm EFF}$ and their errors ϵ_T are listed in Table 3, where we have computed the effective temperature from

$$T_{\rm EFF} = 1.316 \times 10^7 \left(\frac{F_{\rm TOT}}{\theta_R^2} \right)^{1/4} K. \quad (2)$$

$F_{\rm TOT}$ is the bolometric flux, corrected for interstellar reddening (in W cm^{-2}) and θ_R is the Rosseland mean stellar angular diameter (in mas). The error in $T_{\rm EFF}$ is obtained from the errors in the total flux ϵ_F and in the angular diameter ϵ_θ through the relationship

$$\frac{\epsilon_T}{T_{\rm EFF}} = \left[\frac{1}{16} \left(\frac{\epsilon_F}{F_{\rm TOT}} \right)^2 + \frac{1}{4} \left(\frac{\epsilon_\theta}{\theta_{\rm UD}} \right)^2 \right]^{1/2}. \quad (3)$$

The errors in the angular diameters are listed in Table 3. The error in the bolometric flux density was assumed to be an average for the entire sample of stars, dependent upon several factors. First, there are errors which depend upon the photometric system and upon the intrinsic variability of the stars observed. Most of our program stars are small-amplitude variable stars. We attempted to establish a reasonable level for the variability (and dispersion for different observers) from infrared data compiled by Gezari *et al.* (1993) for similar kinds of stars, but not necessarily the same ones observed for this program. This was necessitated by the fact that, often, very few repeated observations existed in the *Catalog of Infrared Observations* for our program stars. From a sample of 268 repeated 2.2 μm observations of nine small-amplitude variable K and M giants and supergiants, we determined the relative error in the flux density to be ± 0.08. Second, there are errors caused by misestimates of the reddening which may result from errors in the measured color, errors in the assigned spectral type or errors in the intrinsic color scale. We tried to evaluate this source of error by scrutinizing those stars in our sample that lie at galactic latitude $b \geq 40°$, where interstellar reddening should (statistically) be small. Seven stars in our sample satisfied this criterion, for which we computed the color difference $\Delta = (B-V) - (B-V)_0$. The mean value of the difference was 0.01, confirming that the mean color excess for the group is low, and the rms value was 0.09. Thus, we adopt an uncertainty of 0.1 in the reddening, and have not applied any corrections to the observed fluxes for stars with $E(B-V) \leq 0.1$. Third, there are uncertainties resulting from errors in the flux calibration. Following Blackwell & Lynas-Gray (1994), we estimate the error from this source to by ± 0.05. Summing all three contributions together in quadrature yields ± 0.14; we adopt ± 0.15 as a conservative average for the sample.

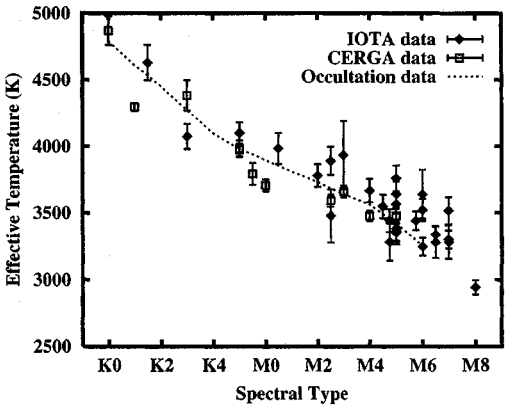

FIG. 2. A plot of the effective temperature measurements for K and M giant stars, made by IOTA and CERGA, as a function of spectral type. For comparison, the effective temperature scale determined by Ridgway *et al.* (1980) is shown as a dotted line.

A few of the stars in our sample are not very well resolved and these tend to have large errors in the effective temperatures. However, there are 34 stars listed in Table 3 with estimated errors less than about 250 K; 29 of these are giants of luminosity class II or III and the remaining five are supergiants. In Fig. 2 we have plotted the 29 highest-precision giant star effective temperatures as a function of spectral type, where the data are shown as filled diamonds (♦). For comparison, we have included the temperatures measured at CERGA, represented by open squares (□), and the mean effective temperature relationship determined by Ridgway *et al.* (1980), shown as a dotted line. The first conclusion from this study is that results from all three methods agree

TABLE 4. Supplemental occultation angular diameters and effective temperatures.

BS	Star	Spectral type	F_{TOT} (W cm^{-2})	θ_R (mas)	ϵ_θ (mas)	T_{EFF} (K)	ϵ_T (K)
1407	75 Tau	K1 III	4.15E-14	2.36	0.25	3866	210
1845	119 Tau	M2 Iab-Ib	5.4E-13	9.83	0.07	3598	45
3357	θ Cnc	K5 III	7.23E-14	3.27	0.13	3773	87
3461	δ Cnc	K0 IIIb	1.01E-13	2.55	0.27	4645	250
...	SW Vir	M7 III:	7.46E-13	17.00	0.11	2966	36
...	HD 142804	M1.5 III	5.94E-14	2.67	0.17	3976	135
6134	α Sco	M1.5 Iab-Ib	8.73E-12	45.65	2.75	3348	108
8850	χ Aqr	M3 III	2.51E-13	6.07	0.16	3780	67

very well. Our detailed comparison of the combined mean Michelson interferometry data with the Ridgway *et al.* scale, indicates that there is an rms difference of about 2% over the entire range, but that the difference is substantially greater than the dispersion in the Michelson data only at two spectral types. We conclude that the agreement between the combined Michelson interferometry temperatures and the occultation temperatures is essentially perfect.

The agreement indicated in Fig. 2 suggests that we may reasonably compare all the available effective temperature estimates from occultations and Michelson interferometry. We have taken the 20 best-determined stars (errors$\leqslant$250 K) from Ridgway *et al.* (1980) and added to them additional published results from the Kitt Peak occultation program. Restricting this latter sample to stars which have spectral types assigned by Morgan & Keenan (1973), Keenan & McNeil (1989) or the *Bright Star Catalog*, we obtain eight additional stars (six of which are giants) with errors $\leqslant$250 K, the parameters for which are summarized in Table 4. The bolometric fluxes for the stars in Table 4 were determined in approximately the same manner as those in Table 1, except in many cases new, unpublished photometry were obtained. We could, in principle, also add the optical wavelength data from the Mark III interferometer (e.g., Hutter *et al.* 1989; Mozurkewich *et al.* 1991), but effective temperatures were not published for those angular diameter measurements.

We have combined together the 66 occultation and near-infrared Michelson interferometry temperature determinations for giant stars to determine the "best" estimates for the mean effective temperatures as a function of spectral type. The procedure was to bin the data in spectral subclasses and form an unweighted mean value. Within each bin, we kept track of the values of the differences, ΔT, between individual temperature determinations and the mean. Then, in order to smooth the data, we performed a boxcar averaging operation across the spectral types, taking ± 1 spectral subtype as the width of the boxcar filter. The results of this averaging and smoothing procedure are listed in Table 5, where we have also listed the older effective temperature scales of Ridgway *et al.* (1980) and DiBenedetto & Rabbia (1987). Determining precise errors for each spectral subtype mean temperature is difficult because of the smoothing procedure. However, we may obtain a reasonable estimate of the average error by considering the distribution of differences, ΔT, which we find to be approximately Gaussian. Taking the rms value of the 53 differences, we find $\Delta T_{rms} \approx 145$ K. There is an average of 2.4 stars per spectral type bin, so that an average error for each effective temperature estimate may be taken to be $\epsilon_T = \Delta T_{rms}/\sqrt{2.4} \approx 95$ K. We adopt 95 K as the uncertainty at each spectral type for our new, mean effective temperature scale.

The natural spread in the effective temperatures at a given spectral class is astrophysically interesting. We measure $\Delta T_{rms} \approx 145$ K, which must consist of at least three components: (1) The natural dispersion; (2) the observational error in measuring the effective temperature, and (3) The observational error in determining the spectral class. We may estimate the second of the errors listed above by taking the rms value of the errors assigned to each individual effective temperature determination. For the stars in the combined sample this results in about ± 120 K. Trying to estimate the error in the spectral class is more difficult. Gliese (1973) has looked at the variation in MK spectral classification for K dwarf stars in the literature and has found a dispersion of ± 0.6. For the sake of further analysis, we assume that this value is representative of the classification errors for the stars presently under consideration. The average slope for the K and M giants is roughly 120 K/spectral class, so that a dispersion of ± 0.6 spectral types would correspond to a dispersion of temperature of about ± 70 K. Subtracting these last two sources of error in quadrature from the measured dispersion, we find that the natural dispersion in the effective temperature could be as small as about ± 40 K. In fact, the errors in

TABLE 5. The mean effective temperature scale.

	Mean effective temperature scale (K)		
Spectral type	This work	Ridgway *et al.* (1980)	DiBenedetto & Rabbia (1987)
K1 III	4510	4610	...
K2 III	4370	4450	...
K3 III	4230	4270	4280
K4 III	4090	4095	4115
K5 III	3920	3980	4000
M1 III	3835	3810	3715
M2 III	3740	3730	3685
M3 III	3675	3640	3630
M4 III	3595	3560	...
M5 III	3470	3420	...
M6 III	3380	3250	...
M7 III	3210	...	...

Note to TABLE 5

The estimated uncertainty for the effective temperatures determined in this paper is ± 95 K for each spectral type.

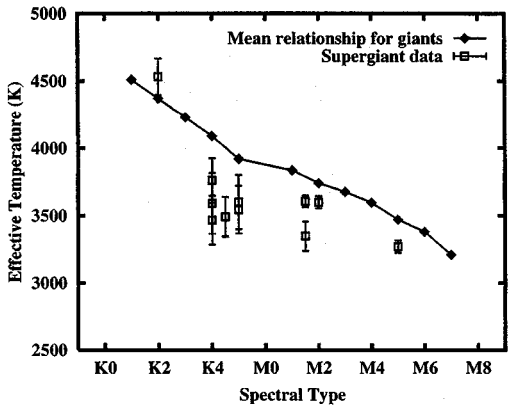

FIG. 3. A comparison of the supergiant effective temperatures to the mean effective temperature vs spectral type relationship for giant stars. The line simply connects the mean points for the giant temperature scale but has no other significance.

spectral type are undoubtedly smaller than the value we have used, since the types have come from one principal source. If there were no errors at all in the spectral type, then the natural dispersion would be about ±80 K. The true value probably lies between these two estimates.

There are fewer stars among luminosity classes I and I-II, so that a detailed analysis is not justified. However, in Fig. 3 we compare the available supergiant effective temperature data to the mean relation for giants just established. It is clear that most of the supergiants lie well below the mean giant data, with the one exception being ϵ Peg. The second conclusion of this work is to confirm our previous results (Dyck *et al.* 1992) for the higher luminosity stars, namely, that they are cooler at a given spectral type than their giant counterparts. Further, one can see a general decline of the temperature difference with advancing spectral type. Combining the IOTA and CERGA data, there are four K supergiants with spectral types between K4 and K5 (averaging slightly warmer than K4.5); taking mean values, we find $T_{\rm EFF}$=3588 K at this spectral type. From our mean relationship at K4.5, we find an average effective temperature $T_{\rm EFF}$=4005 K. Thus, the luminosity class I stars are roughly 400 K cooler than their luminosity class III counterparts at spectral type K4.5. Between spectral types M1 and M2, there are three supergiants in the IOTA and supplemental occultation sample, which average slightly cooler than M1.5. Our relationship predicts a mean giant temperature of 3760 K, about 240 K warmer than the three supergiants. Our lone supergiant at M5, α Her, is 200 K cooler than the M5 giants, but only lies about 1.5 times the combined errors away from the mean value for the giants. At present we have no explanation for the position of ϵ Peg in the H–R diagram. We have checked the spectral type and there seems to be no possibility of a misclassification in luminosity. Further, if there were an unseen double star in the field of view of the interferometer, the effect would be to reduce the visibility, increase the angular diameter and lower the effective temperature, opposite to the observed effect. This star will require more detailed study to understand the observations.

TABLE 6. Estimates of mean linear radii.

Spectral type	$R^*/R_\odot$
K1 III	16±2
K4 III	31±6
M0 III	40±2
M4 III	83±19

4. LINEAR RADII

With the newly determined angular diameters, it is tempting to hope that there are existing parallax data which would allow one to compute linear radii. In fact, the supergiants are beyond the range of classical ground-based astrometric capabilities and very few of the giants have well-determined parallaxes. Nevertheless, we have correlated the angular diameter data from IOTA, CERGA, the Mark III, and occultations with the best parallaxes in the *General Catalogue of Trigonometric Stellar Parallaxes* (Jenkins 1963). Twenty-two stars were found with parallaxes, $\pi \geqslant 3\ \epsilon_\pi$, where ϵ_π is the measurement error. Because many of these parallaxes are only three to four times the error, we have binned the observations into spectral type ranges K0–K2 (mean K1), K3–K5 (mean K4), K7–M0.5 (mean M1), and M2–M6 (mean M4). The estimated error for each mean spectral type is the standard deviation of the mean of all values within the spectral type range. The results are listed in Table 6 as $R_*/R_\odot$, the ratio of the stellar radius to the Solar radius. We note, as expected, that there is a general increase of the size of giants as one progresses toward the cooler types, with about a factor of 2 increase in size for each decrease of 500 K in the effective temperature. We have compared our estimates of stellar sizes to those given by Schmidt-Kaler (1982) and find the agreement reasonable at the hotter types. To our knowledge there have been no published estimates of linear radii for giants later than early M. However, when the Hipparchos data are available there should be a dramatic increase in high-quality parallaxes, so that linear stellar scale sizes will be well determined to at least M8.

5. ESTIMATING APPARENT ANGULAR DIAMETERS

In this paper we have focused on the determination of stellar effective temperatures based on measured angular diameter and photometry. It is often desired to invert this process and estimate the angular diameter based on photometry and $T_{\rm EFF}$ calibrations. A convenient procedure is to use published compilations of spectrophotometry to estimate the bolometric flux and to use a $T_{\rm EFF}$ versus spectral type calibration along with Eq. (2) to compute the limb-darkened diameter. We have carried out this calculation and present the results in Table 7 in the form of Rosseland mean angular diameter (in mas) for a star of K magnitude zero. For convenient reference, we have carried out this calculation for earlier spectral types as well as those discussed in this paper. The types earlier than G are based on intensity interferometry results (Hanbury Brown *et al.* 1974). The G stars are

TABLE 7. Rosseland mean angular diameters versus spectral type for $K=0$.

Spectral type	θ_R (mas)	Spectral type	θ_R (mas)
B0	1.92	M0	5.64
A1	3.21	M1	5.78
F0	3.61	M2	5.87
F8	4.35	M3	5.95
G8	4.68	M4	5.98
K0	4.75	M5	6.10
K1	4.98	M6	6.60
K2	5.22	M7	7.11
K3	5.32	M8	(7.9)
K4	5.47	M9	(8.4)
K5	5.54	M10	(8.8)

based upon the results in Ridgway *et al.* (1980) and the K0 through M7 stars are based upon the $T_{\rm EFF}$ calibration presented in this paper. Stars later than M7 are merely an extrapolation of the latter calibration and are only included as preliminary estimates which may be useful in planning observations.

In order to predict an observational result from Table 7, it will be necessary to multiply the Rosseland mean angular diameter by a limb-darkening correction to yield an appropriate uniform disk angular diameter. The correction will be wavelength dependent, but typically in the range 0.8–1.0. We expect that the apparent diameters estimated in this way will be useful as guides and may not be accurate to more than about 10% over the visible and near-infrared parts of the spectrum.

6. CONCLUSION

We have shown that it is possible to amass a large quantity of angular diameter data for K and M giants and supergiants, using existing ground-based interferometers. Approximately one-third of such stars available to IOTA have now been observed and new effective temperatures computed. From an analysis of the statistics of these temperatures, we do not believe that further observations in the spectral interval K0 III to M7 III will add much new astrophysical information. A more fruitful investigation would be to concentrate observations on those small-amplitude giant variables with spectral types later than M7, and to push the effective temperature scale to its' ultimate limit in the H–R diagram.

We would like to thank the staff at the Center for Astrophysics for a generous allotment of telescope time so that this project could be carried out. We especially thank Wes Traub and Marc Lacasse for the long hours they put in to replace the old autoguiding CCD detectors which failed in 1994. We also thank the Santa Barbara Instrument Group for the speedy loan of control electronics when one of ours failed. Without both of these efforts, most of these observations would not have been possible. We acknowledge helpful conversations with Wes Lockwood. HMD and JAB are grateful to Sidney Wolff for the hospitality provided to them while they were visiting scientists at NOAO. This research has been partially supported by NSF Grant No. AST-9021181 to the University of Wyoming. This research has made use of the SIMBAD database, operated by the CDS, Strasbourg, France.

REFERENCES

Benson, J. A., *et al.* 1991, AJ, 102, 2091
Blackwell, D. E., *et al.* 1983, MNRAS, 205, 897
Blackwell, D. E., & Lynas-Gray, A. E. 1994, A&A, 282, 899
Carleton, N. P., *et al.* 1994, Proc. SPIE, 2200, 152
DiBenedetto, G. P., & Rabbia, Y. 1987, A&A, 188, 114
DiBenedetto, G. P., & Ferluga, S. 1990, A&A, 236, 449
DiBenedetto, G. P. 1993, A&A, 270, 315
Dyck, H. M., Lockwood, G. W., & Capps, R. W. 1974, ApJ, 189, 89
Dyck, H. M., Benson, J. A., Ridgway, S. T., & Dixon, D. J. 1992, AJ, 104, 1982
Dyck, H. M., *et al.* 1995, AJ, 109, 378
Gezari, D. Y., Schmitz, M., Pitts, P. S., & Mead, J. M. 1993, Catalog of Infrared Observations, NASA Reference Publication 1294
Gliese, W. 1973, in IAU Symposium No. 50, edited by Ch. Fehrenbach and B. E. Westerlund (Reidel, Dordrecht), p. 52
Hanbury Brown, R., Davis, J., & Allen, L. R. 1974, MNRAS, 167, 121
Hayes, D. S. 1984, in Calibration of Fundamental Stellar Quantities, edited by D. S. Hayes, L. E. Pasinetti and A. G. D. Philip (Reidel, Dordrecht), p. 246
Hayes, D. S., & Latham, D. W. 1975, ApJ, 197, 593
Hoffleit, D. 1982, Catalog of Bright Stars (Yale University Press, New Haven)
Hutter, D. J., *et al.* 1989, AJ, 340, 1103
Jenkins, L. F. 1963, General Catalogue of Trigonometric Stellar Parallaxes (Yale University Press, New Haven)
Johnson, H. L. 1966, ARA&A, 4, 193
Johnson, H. L. 1968, in Nebulae and Interstellar Matter, edited by B. M. Middlehurst and L. H. Aller (University of Chicago Press, Chicago), Chap. 5
Keenan, P. C. 1942, ApJ, 95, 461
Keenan, P. C. 1963, in Basic Astronomical Data, edited by K. Aa. Strand (University of Chicago Press, Chicago), Chap. 8
Keenan, P. C. & McNeil, R. C. 1989, ApJS, 71, 245
Kukarkin, B. V., *et al.* 1969, General Catalogue of Variable Stars, Third Edition (Astronomical Council of the Academy of Sciences in the USSR, Moscow)
Lockwood, G. W. 1972, ApJS, 24, 375
Mathis, J. S. 1980, ARA&A, 28, 37
Moore, J. H., & Paddock, G. F. 1950, ApJ, 112, 48
Morgan, W. W., & Keenan, P. C. 1973, ARA&A, 11, 29
Mozurkewich, D., *et al.* 1991, AJ, 101, 2207
Ridgway, S. T., Joyce, R. R., White, N. M., & Wing, R. F. 1980, ApJ, 235, 126
Schmidt-Kaler, Th. 1982, in Landolt-Börnstein New Series, Volume 2b, Astronomy and Astrophysics—Stars and Star Clusters, edited by K. Schaifers and H. H. Voigt (Springer, New York)
Scholz, M. 1985, A&A, 145, 251
Scholz, M., & Takeda, Y. 1987, A&A, 186, 200
Tsuji, T. 1978, PASJ, 30, 435
Wright, K. O. 1970, Vistas Astron., 12, 147